Heliyon 10 (2024) e36298

Contents lists available at ScienceDirect

Heliyon

journal homepage: www.cell.com/heliyon

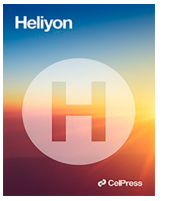

Research article

Targeting TAG-72 in cutaneous T cell lymphoma

Vera J. Evtimov [a,c,*], Maree V. Hammett [a,c], Aleta Pupovac [a,c], Nhu-Y N. Nguyen [a,c], Runzhe Shu [a,c], Carrie Van Der Weyden [a,b], Robert Twigger [b], Ian T. Nisbet [a,c], Alan O. Trounson [a,c], Richard L. Boyd [a,c], H. Miles Prince [b]

[a] *Cartherics Pty Ltd, Notting Hill, Australia*
[b] *Sir Peter MacCallum Department of Oncology, University of Melbourne, Parkville, Australia*
[c] *Australian Regenerative Medicine Institute, Monash University, Australia*

ARTICLE INFO

Keywords:
CAR-T cells
CTCL
TAG-72
CA 72-4

ABSTRACT

Purpose: Current monoclonal antibody-based treatment approaches for cutaneous T cell lymphoma (CTCL) rely heavily on the ability to identify a tumor specific target that is essentially absent on normal cells. Herein, we propose tumor associated glycoprotein-72 (TAG-72) as one such target. TAG-72 is a mucin-associated, truncated O-glycan that has been identified as a chimeric antigen receptor (CAR)-T cell target in solid tumor indications. To date, TAG-72 targeting has not been considered in the setting of hematological malignancies.

Experimental design: $CD3^+$ cells from patients with CTCL were analyzed for TAG-72 expression by flow cytometry. Immunohistochemistry was used to assess TAG-72 expression in CTCL patient skin lesions and a TAG-72 ELISA was employed to assess soluble TAG-72 (CA 72-4) in patient plasma. TAG-72 CAR transduction was performed on healthy donor (HD) and CTCL T cells and characterized by flow cytometry. *In vitro* CAR-T cell function was assessed by flow cytometry and xCELLigence® using patient peripheral blood mononuclear cells and proof-of-concept ovarian cancer cell lines. *In vivo* CAR-T cell function was assessed in a proof-of-concept, $TAG\text{-}72^+$ ovarian cancer xenograft mouse model.

Results: TAG-72 expression was significantly higher on total $CD3^+$ T cells and $CD4^+$ subsets in CTCL donors across disease stages, compared to that of HDs. TAG-72 was also present in CTCL patient skin lesions, whereas CA 72-4 was detected at low levels in both CTCL patient and HD plasma with no differences between the two groups. *In vitro* cytotoxicity assays showed that anti-TAG-72 CAR-T cells significantly, and specifically reduced $CD3^+TAG\text{-}72^+$ expressing CTCL cells, compared to culture with unedited T cells (no CAR). CTCL CAR-T cells had comparable function to HD CAR-T cells *in vitro* and CAR-T cells derived from CTCL patients eradicated cancer cells *in vivo*.

Conclusion: This study shows the first evidence of TAG-72 as a possible target for the treatment of CTCL.

Statement of translational relevance

* Corresponding author. Cartherics Pty Ltd, Notting Hill, Victoria, 3168, Australia.
E-mail address: vera.evtimov@monash.edu (V.J. Evtimov).

https://doi.org/10.1016/j.heliyon.2024.e36298
Received 3 March 2024; Received in revised form 1 August 2024; Accepted 13 August 2024
Available online 22 August 2024

Cutaneous T cell lymphoma (CTCL) is a heterogenous disease that presents with a variety of clinical features. These patients are considered incurable, have limited standard treatment options with inevitable relapse, highlighting a need for novel and more effective therapies. Chimeric antigen receptor (CAR) immune cell therapy is a new pillar of cancer treatment that may deliver more effective treatment options for CTCL, however being a T cell malignancy, there are more challenges than that encountered with B cell malignancies. This study shows, for the first time, that the tumor associated glycoprotein-72 (TAG-72) is expressed on disease $CD4^+$ T cells in CTCL patients and that these cells can be eradicated with TAG-72 CAR-T cells *in vitro*. We subsequently generated CAR-T cells using CTCL donor $CD8^+$ T cells; these were potent killers of human cancer cells transplanted into immune deficient mice. Our preclinical studies outline that TAG-72 is a novel target for CAR-T cell therapy for CTCL.

1. Introduction

Cutaneous T cell lymphoma (CTCL) is a highly diverse form of non-Hodgkin's lymphoma that manifests predominantly in the skin. The most common subtypes are mycosis fungoides (MF) and primary cutaneous $CD30^+$ anaplastic large cell lymphoma. Sezary syndrome (SS), the leukemic form of CTCL, is more rare and accounts for approximately 2–5% of cases [1,2]. SS is defined by tumor cells in the blood and lymph nodes, in addition to skin infiltrates [1]. MF is commonly an indolent CTCL subtype, while SS exhibits more aggressive disease.

Historically, SS was considered a variant of MF, but genomic differences [3,4] and differential marker expression [5–8] suggest they are distinct diseases. Due to CTCL clinical heterogeneity, a standard treatment plan does not exist, but they range from skin-directed therapies for early-stage disease, to systemic chemotherapy and biological therapies for advanced-stage disease or refractory early-stage disease [1]. None of these treatments are curative and response duration is short, typically measured in a few months [9,10]. There is thus a pressing need for novel, strategically targeted effective therapies that ideally target all stages of the disease [1,11].

CAR-T immunotherapy has recently emerged as one such option. It has achieved remarkable outcomes for relapsed/refractory B cell malignancies including acute lymphoblastic lymphoma, large cell B cell lymphoma and myeloma [12–16]. This success has inspired the use of CAR-T cells for other tumor types, but several challenges remain in targeting T cell malignancies including fratricide and T cell aplasia because of shared antigen targets. There is also a risk of life-threatening adverse events such as cytokine release syndrome (CRS). Consequently, there is a need for novel CAR immunotherapies against these T cell malignancies [17], but a primary concern is the identification of relevant target antigens.

Neo-antigenic mutants formed by aberrant glycosylation in tumor cells represent attractive immunotherapeutic targets [18]. The tumor associated glycoprotein-72 (TAG-72, sialyl-Tn) is overexpressed in several epithelial cancers, particularly adenocarcinomas. It is not present in normal adult tissues, other than limited expression in secretory endometrial tissue and rare duodenal goblet cells [19–21]. Preclinical and Phase I studies demonstrate that TAG-72 is a feasible candidate for CAR-T therapy in ovarian and colorectal cancer [22–25]. To the best of our knowledge, TAG-72 expression and its role in CTCL is presently unknown. In this study, we show for the first time that T cells derived from patients with CTCL show increased expression of TAG-72 compared to T cells from healthy human donors (HDs). Specifically, we show that TAG-72 has elevated expression on blood $CD3^+CD4^+$ T cells in patients with various stages of CTCL. Following exposure to our TAG-72 CAR-T cells, the frequency of $CD3^+$TAG-72^+ CTCL cells was greatly reduced *in vitro*. As malignant CTCL T cells are usually a $CD4^+$ phenotype [26], we created functionally cytotoxic CAR-T cells from purified CTCL-derived patient $CD8^+$ T cells. Due to a lack of CTCL mouse models available to assess TAG-72 targeting, we validated the effectiveness of HD and CTCL CAR-T cells *in vivo* by utilizing an ovarian cancer model with known TAG-72 expression [25]. These data suggest a novel, CAR-T targeted approach for combating CTCL.

2. Methods

2.1. Cell lines

All cell lines, including the T cell leukemia cell line Jurkat (ATCC® TIB-152™, RRID: CVCL_0367), the ovarian cancer cell line OVCAR-3 (ATCC® HTB-161™, RRID: CVCL_0465) and the ovarian cancer cell line derived from ascites MES-OV (ATCC® CRL-3272™, RRID: CVCL_CZ92) were acquired from the American Type Culture Collection (ATCC, Manassas, VA, USA) via In Vitro Technologies (Lane Cove West, New South Wales, Australia) and maintained using recommended culture conditions. Ovarian cancer cell lines were utilized as proof-of-concept models for TAG-72 targeting throughout.

2.2. Preparation of peripheral blood mononuclear cells and plasma

Primary human T cells were isolated from HDs either from fresh whole blood or from buffy coats obtained from the Australian Red Cross Lifeblood. The CTCL samples were obtained from Peter MacCallum Cancer Centre and approved by the Human Research Ethics Committee at Monash Health 16055A (Development of Novel Immunotherapies for Cancer). All donors provided informed consent. Peripheral blood mononuclear cells (PBMCs) were separated via Ficoll density centrifugation using Leucosep® tubes (Sigma-Aldrich, St. Louis, MO, USA) within 6 h of blood collection. Matched plasma samples were retained where possible. CTCL patients were grouped into categories based on their assigned clinical stage: IA-IIA were defined as early stage, and IIB-IVB were defined as late stage. CTCL confirmed patients without a known or prescribed clinical stage at the time of sample collection were identified as "unclassified". Refer

to Supplemental Table 1 for diagnosis and disease stage reported on blood collection and/or defined at the time of sample collection. It is important to note that access to detailed patient information was limited by privacy concerns and data availability. Consequently, the scope of disease-specific data presented herein encompasses the entirety of information available to us at the time of the study. We acknowledge this limitation and advise readers to consider this context when interpreting our findings. This study was conducted in accordance with the Declaration of Helsinki.

2.3. Flow cytometry

Transduction efficiency was evaluated by flow cytometry using either green fluorescent protein (GFP), Alexa Fluor® 488 or allophycocyanin (APC) AffiniPure F(ab')₂ Fragment Goat Anti-Mouse IgG, F(ab')₂ fragment specific (Jackson ImmunoResearch Laboratories, Pennsylvania, USA). Frequency of T cell subsets was determined by staining for CD3 fluorescein isothiocyanate (FITC, REA613), phycoerythrin (PE)-Vio®770 (REA613) or Vio®Blue (REA613), CD4 Vio®Blue (VIT4) or Vio®Green (REA623), CD7 PE-Vio®770 (CD7-6B7), CD8 APC (REA734), CD30 Vio®Blue (Ki-2), CC chemokine receptor (CCR)4 APC (REA279), CCR7 Vio®Blue (REA546) and CD45RO APC (REA611); all antibodies were acquired from Miltenyi Biotec (Bergisch Gladbach, Germany). Target antigen expression was characterized using the AlexaFluor® 488-conjugated anti-TAG-72 diabody (Avipep, Parkville, Victoria, Australia) or anti-TAG-72 (CC49) PE (Santa Cruz Biotechnology, Dallas, TX, USA). Staining was performed at 4 °C for 15–30 min. Viability staining employed either VioBility™ 405/520 Dye (Miltenyi Biotec, Bergisch Gladbach, Germany) or Propidium iodide (PI; Sigma, St. Louis, MO, USA; or Miltenyi Biotec, Bergisch Gladbach, Germany). Data were acquired using the MACSQuant® Analyser (Miltenyi Biotec, Bergisch Gladbach, Germany). Subsequent analysis was performed using FlowLogic™ (Inivai Technologies, Mentone, Victoria, Australia).

2.4. Immunohistochemistry

Skin specimens from consenting CTCL patients were immediately fixed in 4 % paraformaldehyde (Sigma-Aldrich, St. Louis, MO, USA). Immunohistochemistry was performed by the Monash Histology Platform at the Monash Health Translation Precinct (Clayton, Victoria, Australia). Formalin-fixed and paraffin-embedded 4 μm sections were stained with primary antibodies against human specific TAG-72 (B72.3, Abcam, Cambridge, United Kingdom) and CD3 (F7.2.38, Abcam, Cambridge, United Kingdom) alongside hematoxylin and eosin (H&E) counterstains using a Dako PT Link and Autostainer (Agilent Technologies, Santa Clara, CA, USA). Images were captured using the Aperio® ScanScope AT Turbo digital slide scanner and associated ImageScope 12.1 software (both Leica Biosystems, Wetzlar, Germany).

2.5. TAG-72 ELISA

Plasma samples from consenting patients and HDs were assessed for soluble TAG-72 using the CA 72-4 ELISA (IBL International, Hamburg, Germany) following the manufacturer's instructions. In brief, samples were incubated with anti-CA 72-4 antibody-horseradish peroxidase conjugate for 2 h at room temperature (RT). Following extensive washing, 3,3′,5,5′-Tetramethylbenzidine was added to all samples and incubated for a further 30 min at RT. The enzymatic reaction was stopped with the addition of 0.5 M H_2SO_4 and absorbance at 450 ± 10 nm was immediately read using SpectraMax® i3 and Softmax® Pro 6.4 software (Molecular Devices, San Jose, CA, USA). Standards and controls were run in parallel. Standard curves were generated and data analyzed using free software at elisaanalysis.com.

2.6. Cytokine array

HD and CTCL patient plasma was stored at −80 °C until required. Samples were subsequently analyzed for secreted human cytokines and chemokines according to the Bio-Plex® Pro™ assay manufacturer's instructions (Bio-Rad, Hercules, CA, USA). In brief, magnetic beads were added to plate wells and washed twice. Standards, blank or samples were added and incubated at RT for 30 min. Plates were washed prior to addition of the detection antibody and then incubated at RT for 30 min. Following washing, streptavidin-PE was added to all wells and incubated at RT for 10 min. A final wash was performed before resuspension in assay buffer. All incubation steps were performed with shaking at 850 rpm. Plates were subsequently read using the Bio-Plex® MAGPIX™ system (Bio-Rad, Hercules, CA, USA). Data were acquired using Bio-Plex® Manager™ MP software and processed using Bio-Plex® Data Pro™ Plus (both Bio-Rad, Hercules, CA, USA).

2.7. CAR construct and lentiviral production

The CAR construct was developed with a single-chain fragment variable (scFv) targeted to TAG-72 [25]. Following a conventional human secretion signal leader, the anti-TAG-72 scFv was constructed in a VH-linker-VL orientation with a 15-residue (Gly4Ser × 3) linker. The CAR construct used human CD8 hinge and transmembrane regions, and 4-1BB and CD3ζ as cytoplasmic signaling domains. In some experiments, the P2A signal sequence directing proteolytic cleavage, was used to direct bicistronic expression of enhanced GFP. In most instances, a second-generation lentiviral packaging system was used to produce the lentiviral vectors. Lentivirus was produced as previously described [25]. Briefly, 293T cells were plated onto poly-l-lysine-coated tissue culture plates (Sigma-Aldrich, St. Louis, MO, USA). The lentiviral transfer vector DNA, together with packaging and envelope plasmid DNA, was transfected with

Lipofectamine™ 2000 (Invitrogen, Carlsbad, CA, USA). Viral supernatant was collected after 48 h and cleared by centrifugation followed by 0.45 μm filtration (Millipore, Burlington, MA, USA). Concentration by ultracentrifugation (120 min at 20,000×*g*) was performed with a Hitachi V100X preparative ultracentrifuge (VWR International, Radnor, PA, USA). Virus pellets were resuspended in PBS and stored at −80 °C until use.

2.8. CAR-T cell production

PBMCs were extracted from HD and CTCL donor whole blood or buffy coat as described above. T cell activation and transduction were performed as previously described [25]. Briefly, freshly thawed PBMCs were enriched for CD4 or CD8 T cells using either the $CD4^+$ and/or $CD8^+$ MicroBead kits (Miltenyi Biotec, Bergisch Gladbach, Germany). Resultant cells were co-cultured with TransAct™ (Miltenyi Biotec, Bergisch Gladbach, Germany) in initiation media comprising of TexMACS™ (Miltenyi Biotec, Bergisch Gladbach, Germany) supplemented with 5 % human AB serum (hAB; Sigma-Aldrich, St. Louis, MO, USA) and 20U/mL recombinant human interleukin (IL)-2 (Miltenyi Biotec, Bergisch Gladbach, Germany) at 1×10^6 cells/mL. Following 24 h, T cells plus TransAct™ (Miltenyi Biotech, Bergisch Gladbach, Germany) were incubated with lentiviral particles and 100U/mL IL-2 on RetroNectin® (Takara Bio, Kusatsu, Japan) coated plates at a multiplicity of infection of 1–2 for an additional 48 h. Activation and transduction were stopped by removal of TransAct™ and lentivirus by centrifugation at 300*g* for 15 min at RT. The cell pellets were resuspended in T cell expansion medium comprising of TexMACS™ containing 20U/mL IL-2, 5 ng/mL IL-7, 5 ng/mL IL-15, 0.1 mg/mL IL-21 (Miltenyi Biotec, Bergisch Gladbach, Germany), 5 % hAB serum (Sigma-Aldrich, St. Louis, MO, USA) and 5 % platelet lysate (Cook Regentec, Indianapolis, IN, USA) at a concentration of 0.5×10^6 cells/mL for expansion. CAR-T cells were expanded for up to 14 days, where approximately every 48 h, the cell concentration was adjusted to 0.5×10^6 cells/mL. On day 7, the transduction efficiency was assessed by either GFP or anti-$F(ab')_2$ expression by flow cytometry. Following expansion, assessment of the T cell phenotype and CAR expression was performed and cells cryopreserved for *in vivo* assessment. In some instances, after at least 7 days of expansion, CAR^+ cells were isolated using the MACSQuant® Tyto® (Miltenyi Biotec, Bergisch Gladbach, Germany).

2.9. In vitro T cell cytotoxicity

The real-time cell analysis instrument xCELLigence® (ACEA Biosciences, San Diego, CA, USA) was utilized to assess T cell killing *in vitro*. Adherent target cells (OVCAR-3 or MES-OV) were plated in 96-well electronic microtiter plates (ACEA Biosciences, San Diego, CA, USA) and allowed to attach for 6–10 h before addition of effector cells at an effector-to-target ratio (E:T) of 5:1 as previously described [25]. T cell (no CAR) control effector cells were analyzed in parallel. Cell impedance was monitored at 15 min intervals for 20 h from the addition of effector cells. All data were normalized to the time of addition of effector cells unless otherwise stated and are presented herein as the arbitrary unit normalized cell index (CI). CAR-T cell function was calculated as % cytotoxicity = [(normalized $CI_{\text{target cells alone}}$ − normalized CI_{test}) ÷ normalized $CI_{\text{target cells alone}}$] × 100.

Since CTCL are non-adherent, the ability of TAG-72 CAR-T cells to kill them *ex vivo* was determined by a reduction in TAG-72 positive cells by flow cytometry. TAG-72 CAR-T cells were added to patient PBMCs at an E:T of 5:1 and maintained in T cell expansion medium for 24–48 h at which point phenotypic analysis was performed. HD PBMCs were maintained in co-culture and analyzed in parallel. All samples were de-identified prior to analysis and experimenters were blinded to the status of test samples throughout the experiment.

2.10. In vivo tumor studies

All animal experiments were pre-approved by the Monash Medical Centre Animal Ethics Committee (MMCA/2018/04, MMCA/2021/05). All procedures followed the National Health and Medical Research Council of Australia guidelines for the use and care of experimental animals. *In vivo* models were established using female 6- to 12-week-old NOD scid gamma (NSG) mice either purchased from Animal Resource Centre (Murdoch, WA, Australia) or bred in in-house colonies (Monash Animal Research Platform, Clayton, Victoria, Australia). OVCAR-3 (1×10^7) cells were prepared in 100 μL of PBS combined with an equal volume of Matrigel™ (Corning Life Sciences, NY, USA) and injected subcutaneously into the back flank. OVCAR-3 tumors were allowed to reach at least 100 mm^3 before treatment commenced. Mice were randomized into experimental groups (3–6 mice/group). Two injections of 5×10^6 CAR-T cells/injection were administered intravenously at 5-day intervals. Control mice received T cells (no CAR) at comparable dosages and intervals. Tumor volume and other clinical parameters of animal health were monitored regularly until experimental endpoint (1000 mm^3 tumor size or morbidity) following initial CAR treatment. Tumors were measured using digital calipers; tumor volumes were calculated using ($width^2 \times length$)/2 (mm^3). At experiment end, mice were euthanized by CO_2 inhalation.

2.11. Statistical analysis

Values represent mean ± standard deviation (SD) for at least three independent experiments unless otherwise stated. Welchs' *t*-test was implemented for comparison of two independent groups. One-way ANOVA analysis with Welch and Brown Forsyth correction was performed for multiple comparison tests unless otherwise stated. Significance was defined as $p \leq 0.05$ and denoted as: *$p \leq 0.05$, **$p \leq 0.01$, ***$p \leq 0.001$ or ****$p \leq 0.0001$. Analysis was performed using GraphPad Prism 8 software (San Diego, CA, USA).

3. Results

3.1. Characterization of TAG-72 expression in T cells isolated from CTCL patients

TAG-72 is well known as a tumor marker of adenocarcinomas [27–29], but to date its expression has not been associated with hematological cancers including CTCL. Therefore, we first determined if TAG-72 expressing cells could be detected in the PBMCs of CTCL patients. Circulating $CD3^+$ T cells from patient PBMCs showed an increased frequency of TAG-72 expression compared to HD $CD3^+$ T cells (Fig. 1A, Supplemental Fig. 1). To determine whether TAG-72 expression differed between disease stages, patients were grouped as early or late stage. TAG-72 expression on circulating $CD3^+$ T cells was significantly higher at all stages of CTCL compared to HD $CD3^+$ T cells, but did not differ significantly between stages (Fig. 1B). Additionally, we did not observe TAG-72 expression on $CD3^{neg}$ cells (Supplemental Fig. 1). Given that the leukemic form of CTCL almost always involves $CD4^+$ cells [26], we assessed differences in TAG-72 expression on circulating $CD4^+TAG\text{-}72^+$ and $CD8^+TAG\text{-}72^+$ T cell subsets. $CD4^+TAG\text{-}72^+$ T cells were significantly higher in CTCL patient samples compared to HD samples, whereas no difference in frequency of $CD8^+TAG\text{-}72^+$ T cells was observed between the groups (Fig. 1C). Circulating CTCL cells are typically $CD4^+CD7^-$ and we classified these as containing the neoplastic population [30]; we observed significantly higher TAG-72 mean fluorescence intensity (MFI) on neoplastic compared to non-neoplastic cells (Fig. 1D). CCR4 and CD30 are recognized targets for CTCL therapy (for example targeted by mogamulizumab and brentuximab vedotin, respectively) [17]. Accordingly, we compared the expression of TAG-72 to that of CCR4 and CD30 on neoplastic cells and found that TAG-72 expression was significantly higher compared to the expression of both these molecules (Fig. 1E).

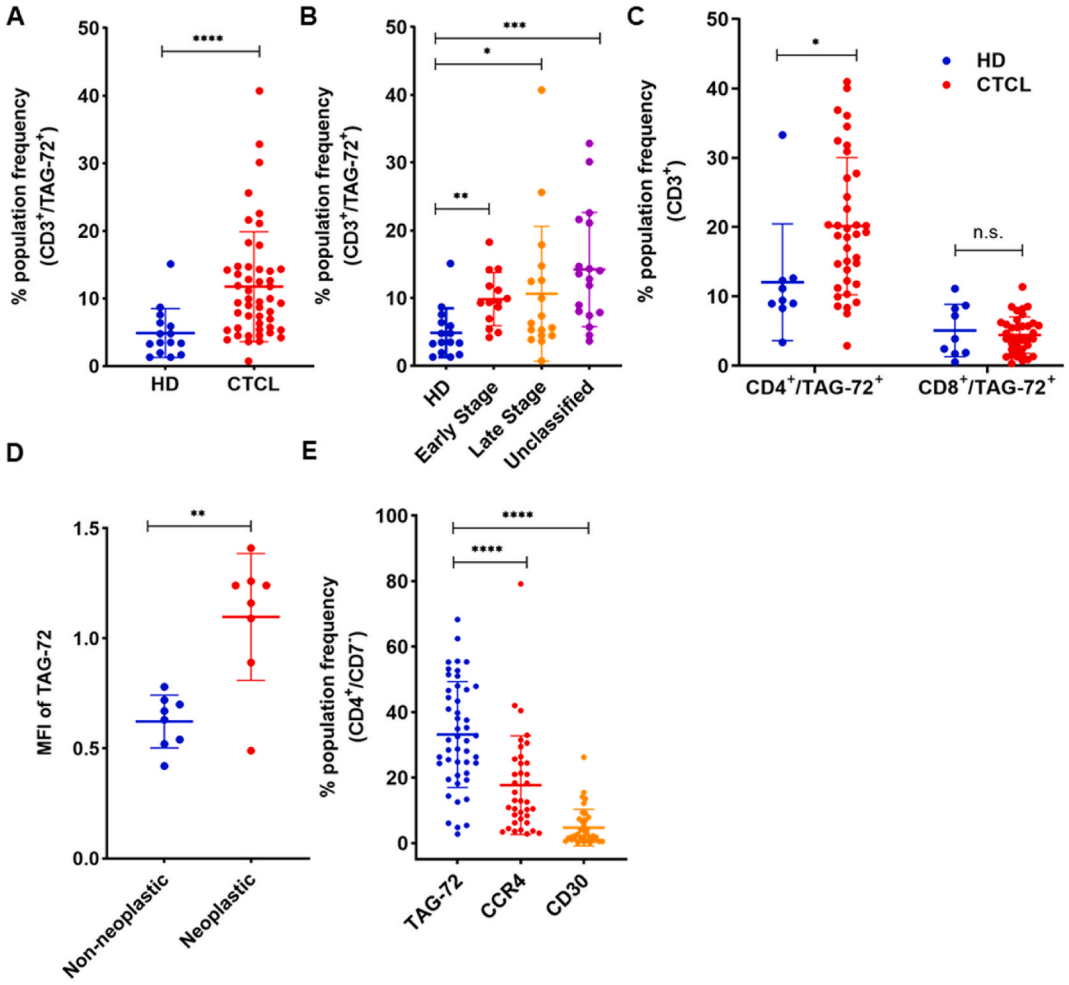

Fig. 1. TAG-72 expression is increased on circulating $CD3^+$ T cells from CTCL patients. (A) The population frequency (%) of circulating $CD3^+TAG\text{-}72^+$ cells from all HDs (blue), all CTCL patients (red), and (B) CTCL patient samples grouped into those with early (red), late (orange) and unclassified (purple) stages of disease. (C) Population frequency (%) of circulating $CD4^+TAG\text{-}72^+$ and $CD8^+TAG\text{-}72^+$ in HD (blue) and CTCL (red) patient samples. (D) TAG-72 expression (MFI) on non-neoplastic (blue) and neoplastic (red) CTCL T cells. (E) Population frequency (%) of TAG-72 (blue), CCR4 (red) or CD30 (orange) expressing neoplastic T cells in CTCL patient samples. Data are represented as the mean ± SD ($n \geq 8$). *$p \leq 0.05$, **$p \leq 0.01$, ***$p \leq 0.001$, ****$p \leq 0.0001$, n.s: not significant.

3.2. Characterization of soluble TAG-72 in CTCL patient plasma and skin lesions

If CAR targeted molecules are present as soluble antigens in patient blood plasma, the efficacy of CAR-T cell therapy may be compromised by binding to the scFv [31]. The presence of soluble TAG-72 in CTCL patient plasma was therefore assessed; the levels in CTCL patient plasma were similar to HD plasma (Fig. 2A). Likewise, when samples were grouped into early, late or unclassified stages, CTCL patient plasma TAG-72 levels remained similar to HD levels (data not shown). CTCL typically presents in the skin, therefore TAG-72 and CD3 presence were determined in skin lesion samples. TAG-72 and CD3 were both detected in CTCL patient skin lesions indicative of infiltration of TAG-72$^+$ T cells (Fig. 2B). However, since these were not on the same biopsy section, further confirmation of the presence of TAG-72$^+$ T cells is required.

3.3. Characterization of CD8$^+$ TAG-72 CAR-T cells

The presence of increased pro-inflammatory cytokines and chemotactic factors in the patient circulation may increase the risk of CRS and/or neurotoxicity after CAR-T cell treatment [32]. Therefore, we compared the plasma cytokine and chemokine levels of HD and CTCL patient samples. There were no increases in pro-inflammatory or chemotactic factors in CTCL patient samples compared to HD samples (Supplemental Fig. 2). Specifically, there was a significant decrease in granulocyte-macrophage colony-stimulating factor (GM-CSF), vascular endothelial growth factor (VEGF), and macrophage inflammatory protein (MIP)-α and increase in the anti-inflammatory factors transforming growth factor (TGF)-β2 and TGF-β3 in CTCL patient plasma compared to HD plasma (Supplemental Fig. 2). This suggests CTCL patient samples utilized herein do not have an elevated cytokine/chemokine profile that may exacerbate CAR-T mediated toxicities. Nonetheless, the absence of this profile does not necessarily guarantee the absence of adverse effects following CAR-T cell therapy.

Malignant T cells in MF and SS are classically a CD4$^+$ phenotype [33], therefore a second-generation TAG-72 CAR was transduced into CD8$^+$ T cells obtained from HD and CTCL patients, to avoid potential activation of blood-derived malignant (CD4$^+$) cells. The CAR contained an anti-TAG-72-specific scFv coupled to a 4-1BB intracellular co-stimulatory domain linked to a CD3ζ signaling domain and

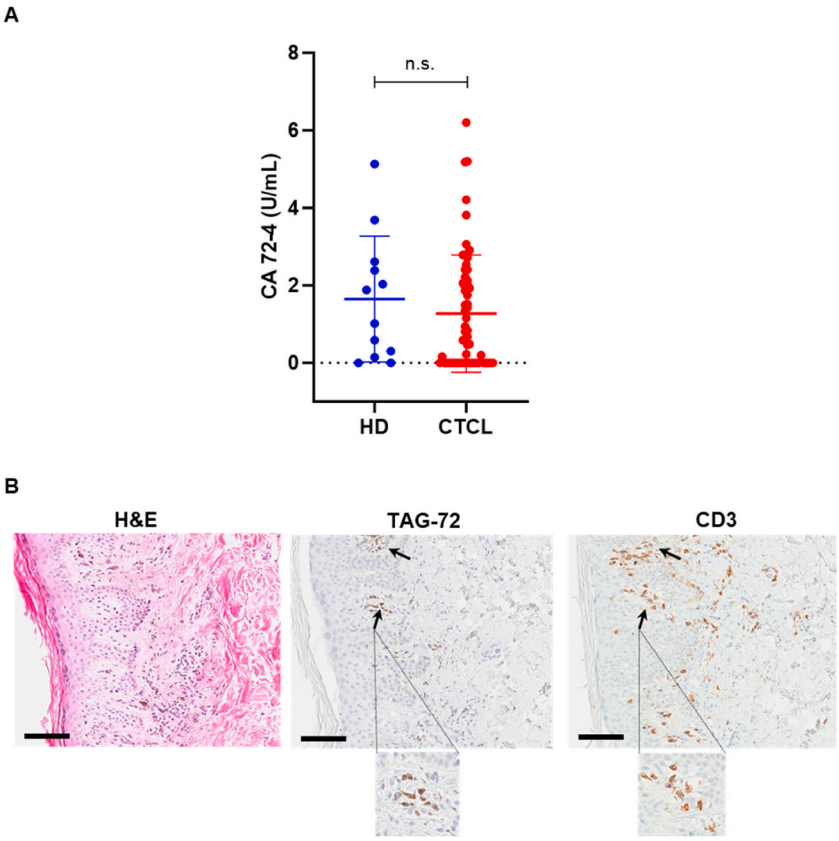

Fig. 2. TAG-72 is present in CTCL patient skin lesions but soluble TAG-72 is not in patient plasma. (A) Soluble TAG-72 (CA 72-4) was quantitated in HD samples (blue) and CTCL patient samples (red). Data are represented as the mean ± SD ($n \geq 12$), no significant (n.s.) differences were observed. (B) Representative H&E staining of a CTCL skin lesion biopsy (left) and immunohistochemistry of TAG-72 (middle) and CD3 (right) expression present in consecutive cryosections. Horseradish peroxidase staining (indicated by arrows and zoomed field of views) indicates the presence of TAG-72 or CD3. Scale bar: 100 μm. Magnification: all images 20×.

a GFP reporter (Fig. 3A). Transduction efficiency, expansion kinetics, prevalent T cell subset phenotype and exhaustion markers were subsequently interrogated. Co-expression of CD8 and the TAG-72 CAR was monitored with comparable transduction observed in $CD8^+$ T cells from HD and CTCL patients (Fig. 3B). TAG-72 CAR-T cells from HD and CTCL patients displayed similar *ex vivo* expansion kinetics (Fig. 3C) and the proportions of T cell subsets remained uniform with effector memory ($CCR7^-/CD45RO^+$) cells, the prevalent phenotype (Fig. 3D). Additionally, the frequency of CAR-T cells expressing the exhaustion markers programmed cell death protein-1 (PD-1), T cell immunoglobulin and mucin domain-3 (TIM-3) and lymphocyte activation gene-3 (LAG-3), remained similar between groups (Fig. 3E). Furthermore, endogenous TAG-72 expression was less than 1 % on $CD8^+$ CAR-T cells after 14 days, suggesting minimal presence of contaminating leukemic cells in the final product (Fig. 3F).

3.4. Functional characterization of $CD8^+$ TAG-72 CAR-T cells

Following phenotypic characterization, we determined whether $CD8^+$ TAG-72 CAR-T cells could eliminate CTCL $CD3^+TAG\text{-}72^+$ T

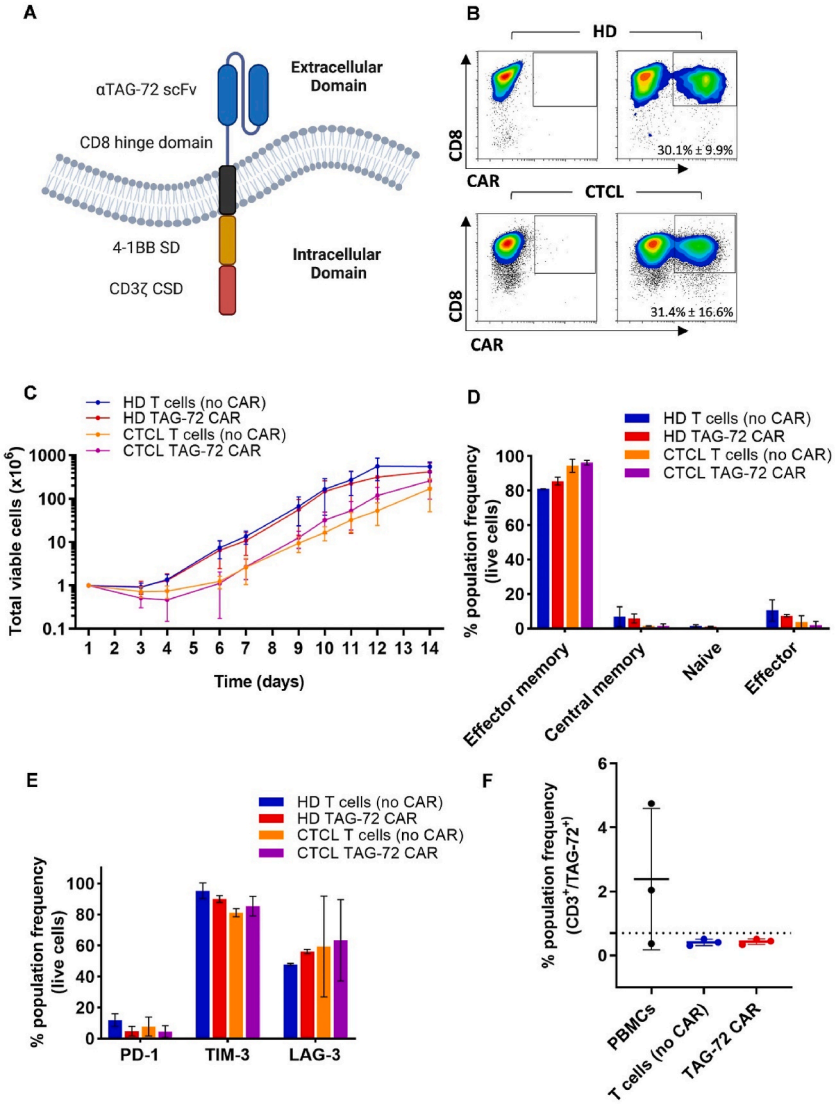

Fig. 3. Characterization of $CD8^+$ TAG-72 CAR-T cells engineered from HD and CTCL patient cells. (A) Schematic representation of the CAR containing an anti-TAG-72 scFv, CD8 hinge, 4-1BB intracellular co-stimulatory domain (CSD) linked to a CD3ζ signaling domain (SD). (B) Transduced T cells (right panels) and T cells (no CAR) (left panels) from HDs and CTCL patients were assessed by flow cytometry to determine transduction efficiency and CD8 expression following cell expansion. (C) Expansion potential of CAR-T cells following transduction. Flow cytometric analysis was used to determine (D) effector memory ($CCR7^-/CD45RO^+$), central memory ($CCR7^+/CD45RO^+$), naïve ($CCR7^+/CD45RO^-$), and effector cell ($CCR7^-/CD45RO^-$) frequency, (E) exhaustion markers PD-1, TIM-3 and LAG-3 in CAR- and T cell (no CAR) controls, and TAG-72^+ cells remaining in the (F) $CD8^+$ CAR-T cell product and its respective controls. Data are represented as mean ± SD (n = 2–5), no significant differences were observed.

cells. Given the abundant expression of TAG-72 on the hematopoetic cell line Jurkat [34], it was utilized as a positive control (Fig. 4A). A significant reduction in frequency and number of $CD3^+TAG\text{-}72^+$ T cells was observed after treatment with TAG-72 CAR-T cells (Fig. 4B and C). This reduction was confirmed by performing cell counts following CAR-T cell and CTCL $CD3^+TAG\text{-}72^+$ T cell co-culture after 24 h (Fig. 4D).

We also compared the cytotoxic function of CTCL CAR-T cells to that of HD cells *in vitro*, by xCELLigence®. Unsorted CAR-T cells ($CD4^+$, $CD8^+$ mixture) were also compared to purified $CD8^+$ CAR-T cells. As expected, CAR-T cells were more potent against $TAG\text{-}72^{hi}$ expressing OVCAR-3 cells (Fig. 5A) compared to $TAG\text{-}72^{lo}$ expressing MES-OV cells (Fig. 5B). Importantly, CTCL CAR-T cells showed equivalent cytotoxicity to that of HD (Fig. 5A–C). Further, there was no significant difference in cytotoxicity between mixed populations of $CD4^+$ and $CD8^+$ CAR-T cells compared to purified $CD8^+$ CAR-T cells (Fig. 5C).

The ability of the $CD8^+$ CAR-T cells to kill cancer cells *in vivo* was examined in NSG mice transplanted subcutaneously with OVCAR-3 cells (Fig. 6A). This OVCAR-3 xenograft model was chosen as a proof-of-concept approach, given the absence of established *in vivo* models for TAG-72 targeting in CTCL. Both HD $CD8^+$ CAR-T cells and CTCL $CD8^+$ CAR-T cells delayed tumor growth (Fig. 6B) and significantly improved survival compared to their respective no-CAR controls (Fig. 6C). Although HD CAR-T cells showed a trend towards improved performance, there was no statistically significant difference in the *in vivo* function between HD CAR-T and CTCL CAR-T cells.

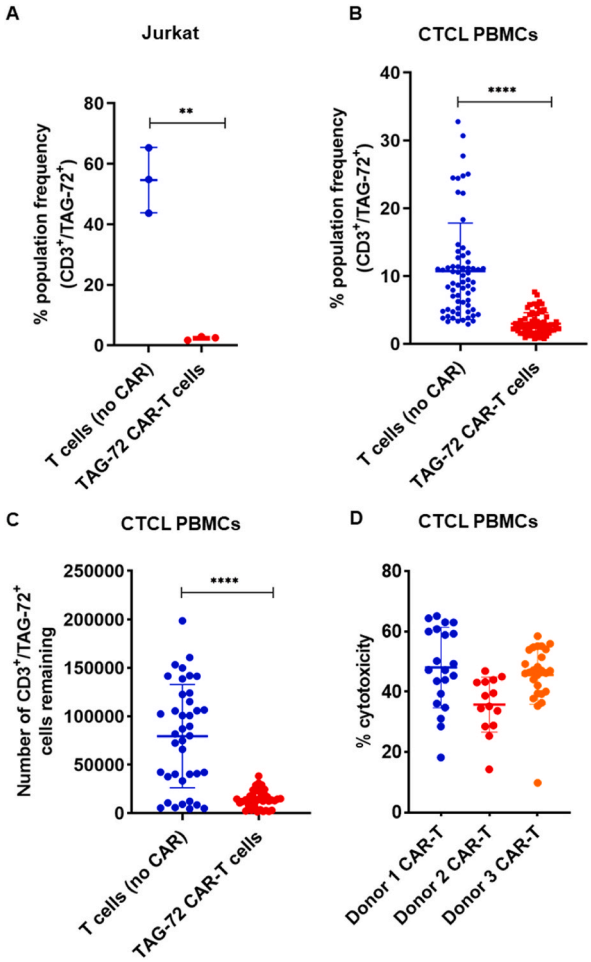

Fig. 4. $CD8^+$ CAR-T cells eliminate $CD3^+TAG\text{-}72^+$ CTCL T cells. (A, B) Population frequency (%) of $CD3^+TAG\text{-}72^+$ cells in (A) $TAG\text{-}72^+$ Jurkat cells and (B) PBMCs from CTCL patients following treatment with TAG-72 CAR-T cells (red) and T cells (no CAR) (blue) at an E:T ratio of 5:1. (C) The number of $CD3^+TAG\text{-}72^+$ cells remaining after treatment of CTCL PBMCs with TAG-72 CAR-T cells (red) and T cells (no CAR) (blue) at an E:T ratio of 5:1. (A–C) Panels display the remaining target cells after co-culturing with CAR-T cells from three different donors. Each matched set of data points (one blue and one red) represents CAR-T cells (red) and their corresponding non-transduced T cell controls (blue) from one of these donors. (D) Percent cytotoxicity (%) was determined by cell counts (derived from data displayed in B and C, relative to T cells (no CAR) control) at the conclusion of 24 h co-culture of CTCL PBMCs and CAR-T cells from 3 different donors as indicated (blue, red and orange). Data are represented as mean ± SD; ($n \geq 3$). $^{**}p \leq 0.01$, $^{****}p \leq 0.0001$.

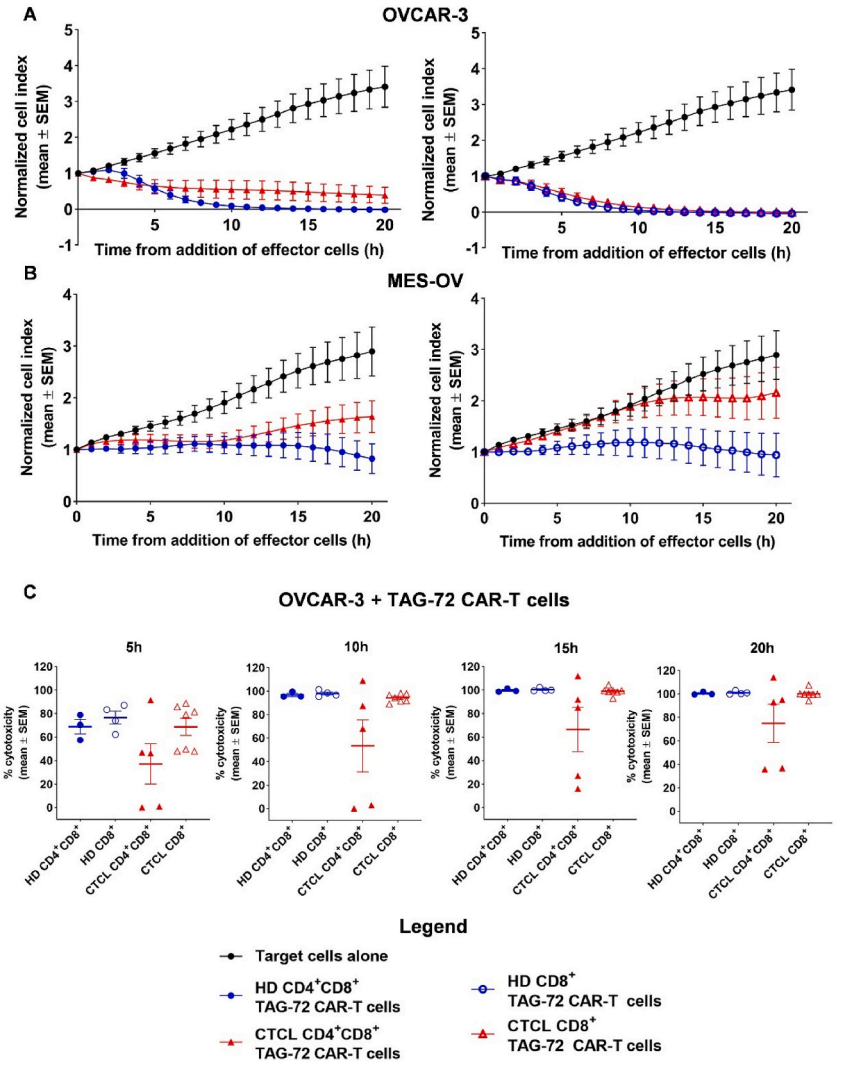

Fig. 5. CTCL CAR-T cells have comparable function to HD CAR-T cells *in vitro*. HD and CTCL $CD4^+CD8^+$ CAR-T cells and $CD8^+$ CAR-T were co-cultured with either OVCAR-3 (A) or MES-OV (B) cell lines at an E:T ratio of 5:1. Target cell response kinetics were measured in real time using xCELLigence® where data represent the average normalized cell index of ≥3 biological replicates ± standard error of mean (SEM). (C) Efficiency of target cell killing was quantitated at 5–20 h (h) of OVCAR-3 and TAG-72 CAR-T cell co-culture (as indicated) and is presented as mean percent cytotoxicity ± SEM. No significant differences were observed.

4. Discussion

Despite the unmet clinical need, CAR-T therapies for T cell malignancies remain problematic largely due the lack of cancer target antigens that don't predispose to the risk of fratricide, product contamination with disease cells and T cell aplasia. TAG-72 is a well-documented CAR-T target for adenocarcinomas, and is absent in most normal tissues [23,29]. A clinical trial has also established the relative safety of TAG-72 CAR-T cells in patients with colon cancer [35]. Additionally, we have previously shown that the CAR design used in this study successfully eradicates ovarian cancer cells *in vitro* and *in vivo* [25]. Here we reveal the unexpected finding that TAG-72 is significantly expressed on $CD3^+CD4^+$ T cells in the blood and present in skin lesions of CTCL patients, with limited expression on HD T cells. TAG-72 expression in the blood was in fact higher than the expression of CCR4 and CD30, two commonly targeted antigens in CTCL using mogamulizumab and brentuximab vedotin, respectively. However, our study does not rule out the possibility that non-neoplastic $CD4^+$ T cells in CTCL patients might exhibit elevated TAG-72 expression levels compared to those found in healthy donors. Such a scenario raises concerns regarding potential undesired off-target effects following CAR-T cell therapy; in this regard we are yet to determine the functional profile of the TAG-72^+ $CD3^+/CD4^+$ cells in healthy donors compared to CTCL patients. Future work should thus elucidate the significance of TAG-72 expression in non-neoplastic $CD4^+$ T cells of these patients. Moreover, it is important to incorporate additional surface markers, such as $CD26^-$ and $CD158k^+$, along with TCR-Vβ repertoire analysis for accurately identifying cancerous cells in CTCL patients and further verifying TAG-72 expression [36]. Understanding these aspects is

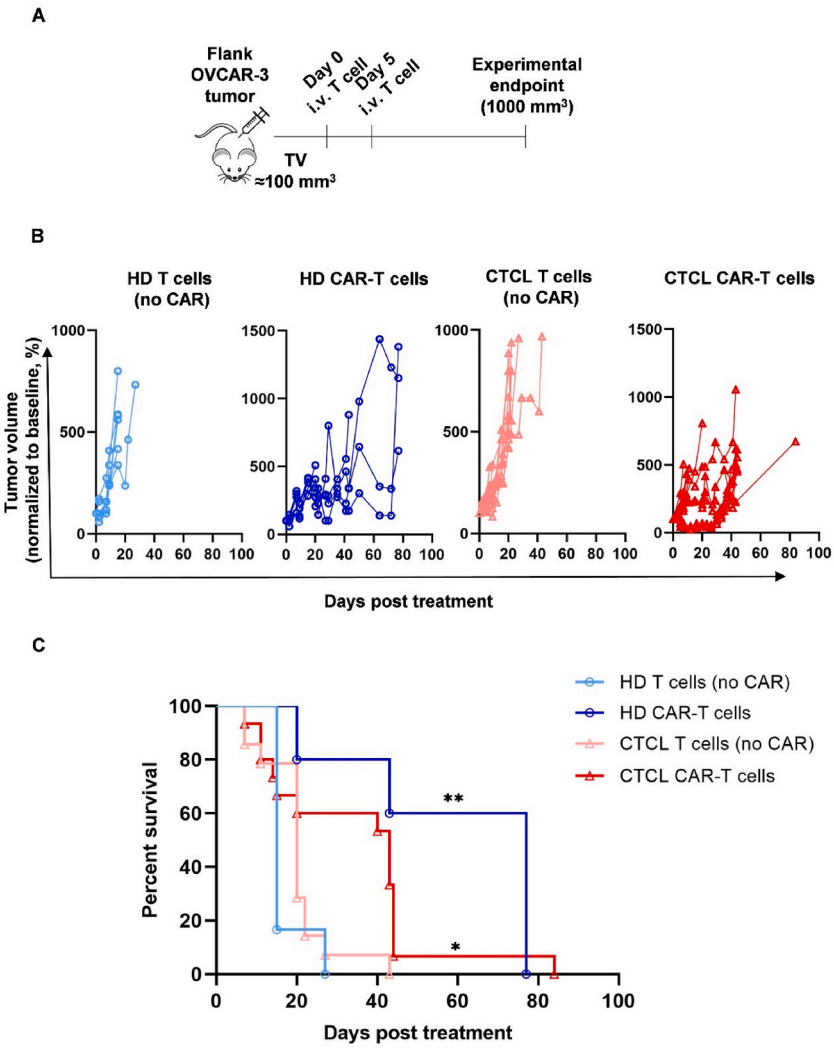

Fig. 6. HD and CTCL CD8$^+$ CAR-T cells demonstrate ability to eliminate cancer cells *in vivo*. (A, B) NSG mice bearing OVCAR-3 derived tumors were treated at 5-day intervals with 5 $\times$ 10^6 HD CD8$^+$ CAR-T cells, CTCL CD8$^+$ CAR-T cells or their respective no-CAR controls with intravenous (i.v.) injection when tumor volume (TV) reached 100 mm$^{3.}$ TV was monitored until experimental end (1000 mm^3). Data were generated using 5–15 mice per treatment and 1–3 T cell donors and are presented as tumor volume normalized to Day 0 baseline (%). (C) Percent survival of mice post T cell infusion as indicated by Kaplan-Meier curve. Survival curves were compared using the Log-rank (Mantel-Cox) test and the Gehan-Breslow-Wilcoxon test. *p $\leq$ 0.05, **p $\leq$ 0.01.

vital for assessing off-target risks associated with CAR-T cell therapy.

Immunohistochemical staining of MF and SS skin lesions shows CD3 positive lymphocytes extending into the mid- and upper-levels of the epidermis [37]. The skin lesion CD3 staining herein mirrors this and additionally shows that some TAG-72$^+$ staining extended beyond CD3$^+$ cells to the extracellular matrix, which may be due to it being shed from the nearby lymphoma cells, or may reflect a cyclic nature of TAG-72 expression. Future studies should incorporate double staining to precisely identify and confirm the presence of tumor cells. By using markers such as PD-1 [38], killer cell immunoglobulin-like receptor 3DL2 [39], thymocyte selection-associated high mobility group box protein [40] and cell adhesion molecule 1 [41], will enhance the understanding of TAG-72 expression in relation to specific tumor cell populations in CTCL. This approach will help to elucidate the role of TAG-72 in disease progression and its potential as a therapeutic target.

We demonstrated the ability to generate functional CAR-T cells from CTCL patients; these had comparable function to HD CAR-T cells *in vitro* and *in vivo*, indicating that even with the clinical condition, patients' T cells are capable of killing tumor cells. In future studies it would be crucial to ascertain how CAR-T cells alter the ratio of malignant to non-malignant cells, or if they affect polyclonal T cells beyond just the clonal malignant cells. Furthermore it would be crucial to understand if CD7$^-$CD26$^-$ and CD158k$^+$ cells are selectively targeted and eliminated by the CAR-T cells. Because the malignant cells are commonly recognized as being within the CD4$^+$ subset [26], we focused on producing CAR-T cells from purified CD8 cells. The prevalent phenotype of these cells were that of effector

memory T cells. Some preclinical studies suggest that central memory T cells provide better anti-tumor responses and that compositions including both CD4 and CD8 cells improve CAR-T cell expansion and persistence [42,43]. Engineering CAR-T cells geared toward a central memory phenotype may improve the anti-tumor capacity of our CAR-T cells, however, the relative importance of the two cell types has not been firmly established in clinical trials. Our *in vitro* data did not show a functional advantage of a composition of T cells versus $CD8^+$ cell alone. Although we did not assess different ratios *in vivo*. The composition of CD4 and CD8 cells also appeared to trend to lower cytotoxicity (not statistically significant) compared to CD8 cells alone. This could potentially reflect a lower proportion of dedicated $CD8^+$ killer cells within the mixed population.To the best of our knowledge, there are no CTCL *in vivo* models utilizing TAG-72 as a target. Therefore to assess the ability of HD and CTCL CAR-T cells to eliminate cancer cells as proof-of-concept *in vivo* we used a well-published model of ovarian cancer with documented high expression of TAG-72 [24,25]. We showed that CAR-T cells derived from both HD and CTCL donors showed equivalent delay of tumor growth and prolonged survival in a xenograft model. However, further optimization and characterization of *in vivo* CAR-T cell killing is required, including assessment of T cell fate such as expansion, persistence, phenotype and ability to achieve complete tumor eradication.

Since soluble TAG-72 (CA 72-4) does not appear to be elevated in CTCL patients' blood, it is unlikely it will interfere with the tumor cell targeting by TAG-72 CAR-T cells. Although CA 72-4 is elevated in the serum of solid tumor patients, and is commonly used in the screening and diagnoses of gastric cancer [44], it is currently unknown whether it is elevated in other hematological cancers.

Patient plasma did not present with significant amounts of cytokines associated with CRS. Additionally, with advancing clinical stage of disease, there is a decline in pro-inflammatory Th1-associated cytokines accompanied with a shift to an anti-inflammatory Th2-associated tumor microenvironment [33]. This suggests patients, at least those at advanced stages of disease, may not have an existing pro-inflammatory environment that may predispose to potential increases in cytokine levels post CAR-T cell treatment. However, further clinical safety investigation is required, especially since CTCL is a highly heterogenous disease and patients present with chronically inflamed skin lesions and different inflammatory environments as disease progresses [45].

Single antigen specific CAR therapies run the risk of cancer escape through mutagenic downregulation of the antigen or epitope being targeted. Indeed our data show that not all $CD3^+$ leukemic cells are TAG-72^+. Nevertheless, we showed the presence of a higher percentage of TAG-72^+ neoplastic cells compared to the well-known and frequently targeted markers, CCR4 and CD30. Additionally, CAR-T cell therapies targeting multiple antigens may improve effectiveness of CTCL therapies [17]. Our previous data show that dual specificity TAG-72- and CD47 CAR-T cells are more effective at killing tumor cells with low expression of target antigen. The CD47 truncated, non-signaling CAR allowed additional targeting without harming normal cells [25]. Such an approach may also be useful in therapeutic targeting of CTCL.

In conclusion, this study reports the novel expression of TAG-72 on CTCL T cells and provides support for CAR targeting of TAG-72 in CTCL.

Data availability

The data used in this study is confidential and not publicly available due to patient privacy.

Ethics statement

All animal experiments were pre-approved by the Monash Medical Centre Animal Ethics Committee (MMCA/2018/04, MMCA/2021/05). CTCL samples were obtained from Peter MacCallum Cancer Centre and approved by the Human Research Ethics Committee at Monash Health 16055A (Development of Novel Immunotherapies for Cancer, May 10, 2016). All donors provided written informed consent.

CRediT authorship contribution statement

Vera J. Evtimov: Writing – review & editing, Writing – original draft, Visualization, Validation, Project administration, Methodology, Investigation, Formal analysis, Data curation, Conceptualization. **Maree V. Hammett:** Writing – review & editing, Writing – original draft, Visualization, Validation, Methodology, Investigation, Formal analysis, Data curation, Conceptualization. **Aleta Pupovac:** Writing – review & editing, Writing – original draft, Visualization, Formal analysis, Data curation. **Nhu-Y N. Nguyen:** Methodology, Investigation, Formal analysis, Data curation. **Runzhe Shu:** Methodology, Investigation. **Carrie Van Der Weyden:** Resources, Methodology. **Robert Twigger:** Resources, Methodology. **Ian T. Nisbet:** Supervision, Resources, Conceptualization. **Alan O. Trounson:** Supervision, Resources, Conceptualization. **Richard L. Boyd:** Supervision, Resources, Conceptualization. **H. Miles Prince:** Supervision, Resources, Conceptualization.

Declaration of competing interest

The authors declare the following financial interests/personal relationships which may be considered as potential competing interests: The research described in this paper was funded by Cartherics Pty Ltd. All authors except H.M.P., C.V.D.W. and R.T, are paid employees of Cartherics and hold options and/or equity in the company. R.L.B, A.O.T and I.T.N are key Cartherics executives and H.M.P. is a member of the company's Scientific Advisory Board. V.J.E, R.L.B, I.T.N, H.M.P and A.O.T are inventors on Cartherics-owned patent applications related to this work.

Acknowledgements

The authors acknowledge Maureen Howard and Peter Hudson for the intellectual contribution that helped shaped the manuscript and Junli Zhuang, Thao Nguyen and Callum Docherty for technical support. The authors acknowledge the staff at Peter MacCallum Cancer Centre for the collection of biological samples and the use of the facilities, equipment and technical assistance of the Monash Histology Platform, Department of Anatomy and Developmental Biology, Monash University and of the Monash Animal Research Platform, Monash University. Fig. 3A was created with BioRender.com. The research described in this paper was funded by Cartherics Pty Ltd.

Appendix A. Supplementary data

Supplementary data to this article can be found online at https://doi.org/10.1016/j.heliyon.2024.e36298.

References

[1] O. Alpdogan, et al., Systemic therapy of cutaneous T-cell lymphoma (CTCL), Chin. Clin. Oncol. 8 (1) (2019) 10–27.
[2] A.C. Hristov, T. Tejasvi, R.A. Wilcox, Mycosis fungoides and Sezary syndrome: 2019 update on diagnosis, risk-stratification, and management, Am. J. Hematol. 94 (9) (2019) 1027–1041.
[3] R. van Doorn, et al., Oncogenomic analysis of mycosis fungoides reveals major differences with Sezary syndrome, Blood 113 (1) (2009) 127–136.
[4] X. Wu, S.T. Hwang, Mycosis fungoides and Sézary syndrome: clinical, immunological and molecular distinctions that suggest two different diseases, Expet Rev. Dermatol. 7 (2) (2012) 181–193.
[5] D.W. Bahler, et al., CD158k/KIR3DL2 is a useful marker for identifying neoplastic T-cells in Sezary syndrome by flow cytometry, Cytometry B Clin Cytom 74 (3) (2008) 156–162.
[6] F. Cetinozman, et al., Differential expression of programmed death-1 (PD-1) in Sezary syndrome and mycosis fungoides, Arch. Dermatol. 148 (12) (2012) 1379–1385.
[7] J.J. Campbell, et al., Sezary syndrome and mycosis fungoides arise from distinct T-cell subsets: a biologic rationale for their distinct clinical behaviors, Blood 116 (5) (2010) 767–771.
[8] C.M. Harro, et al., Sezary syndrome originates from heavily mutated hematopoietic progenitors, Blood Adv 7 (18) (2023) 5586–5602.
[9] C.F. Hughes, et al., Lack of durable disease control with chemotherapy for mycosis fungoides and Sezary syndrome: a comparative study of systemic therapy, Blood 125 (1) (2015) 71–81.
[10] N. Mehta-Shah, et al., NCCN guidelines insights: primary cutaneous lymphomas, version 2.2020, J. Natl. Compr. Cancer Netw. 18 (5) (2020) 522–536.
[11] M. Martinez, E.K. Moon, CAR T cells for solid tumors: new strategies for finding, infiltrating, and surviving in the tumor microenvironment, Front. Immunol. 10 (2019) 128.
[12] S.J. Schuster, et al., Tisagenlecleucel in adult relapsed or refractory diffuse large B-cell lymphoma, N. Engl. J. Med. 380 (1) (2019) 45–56.
[13] F.L. Locke, et al., Long-term safety and activity of axicabtagene ciloleucel in refractory large B-cell lymphoma (ZUMA-1): a single-arm, multicentre, phase 1-2 trial, Lancet Oncol. 20 (1) (2019) 31–42.
[14] S.S. Neelapu, et al., Axicabtagene ciloleucel CAR T-cell therapy in refractory large B-cell lymphoma, N. Engl. J. Med. 377 (26) (2017) 2531–2544.
[15] P. Sharma, et al., FDA approval summary: idecabtagene vicleucel for relapsed or refractory multiple myeloma, Clin. Cancer Res. 28 (9) (2022) 1759–1764.
[16] K.C. Pehlivan, B.B. Duncan, D.W. Lee, CAR-T cell therapy for acute lymphoblastic leukemia: transforming the treatment of relapsed and refractory disease, Curr Hematol Malig Rep 13 (5) (2018) 396–406.
[17] I. Scarfo, M.J. Frigault, M.V. Maus, CAR-based approaches to cutaneous T-cell lymphoma, Front. Oncol. 9 (2019) 259.
[18] E. Rodriguez, S.T.T. Schetters, Y. van Kooyk, The tumour glyco-code as a novel immune checkpoint for immunotherapy, Nat. Rev. Immunol. 18 (3) (2018) 204–211.
[19] A. Thor, et al., Monoclonal antibody B72.3 reactivity with human endometrium: a study of normal and malignant tissues, Int. J. Gynecol. Pathol. 6 (3) (1987) 235–247.
[20] J.A. Nagle, D.C. Wilbur, M.B. Pitman, Cytomorphology of gastric and duodenal epithelium and reactivity to B72.3: a baseline for comparison to pancreatic lesions aspirated by EUS-FNAB, Diagn. Cytopathol. 33 (6) (2005) 381–386.
[21] M. Xu, et al., Expression of TAG-72 in normal colon, transitional mucosa, and colon cancer, Int. J. Cancer 44 (6) (1989) 985–989.
[22] M.G. Rosenblum, et al., *Phase I study of* ^{90}*Y-labeled B72.3 intraperitoneal administration in patients with ovarian cancer: effect of dose and EDTA coadministration on pharmacokinetics and toxicity*, Clin. Cancer Res. 5 (5) (1999) 953–961.
[23] K.M. Hege, et al., Safety, tumor trafficking and immunogenicity of chimeric antigen receptor (CAR)-T cells specific for TAG-72 in colorectal cancer, J Immunother Cancer 5 (1) (2017) 22–35.
[24] J.P. Murad, et al., Effective Targeting of TAG72^{+} peritoneal ovarian Tumors via regional Delivery of CAR-engineered T cells, Front. Immunol. 9 (2018) 2268.
[25] R. Shu, et al., Engineered CAR-T cells targeting TAG-72 and CD47 in ovarian cancer, Mol Ther Oncolytics 20 (2021) 325–341.
[26] S. Nakai, E. Kiyohara, R. Watanabe, Malignant and benign T cells constituting cutaneous T-cell lymphoma, Int. J. Mol. Sci. 22 (23) (2021) 12933–12947.
[27] D. Karan, et al., Expression of tumor-associated glycoprotein-72 (TAG-72) antigen in human prostatic adenocarcinomas, Oncol. Rep. 8 (5) (2001) 1123–1126.
[28] M.P. Ponnusamy, et al., Expression of TAG-72 in ovarian cancer and its correlation with tumor stage and patient prognosis, Cancer Lett. 251 (2) (2007) 247–257.
[29] A. Thor, et al., Distribution of oncofetal antigen tumor-associated glycoprotein-72 defined by monoclonal antibody B72.3, Cancer Res. 46 (6) (1986) 3118–3124.
[30] E.A. Olsen, et al., Clinical end points and response criteria in mycosis fungoides and Sezary syndrome: a consensus statement of the International Society for Cutaneous Lymphomas, the United States Cutaneous Lymphoma Consortium, and the Cutaneous Lymphoma Task Force of the European Organisation for Research and Treatment of Cancer, J. Clin. Oncol. 29 (18) (2011) 2598–2607.
[31] M. Cartellieri, et al., Chimeric Antigen Receptor-Engineered T Cells for Immunotherapy of Cancer, vol. 2010, J Biomed Biotechnol, 2010 956304.
[32] Z. Wang, W. Han, Biomarkers of cytokine release syndrome and neurotoxicity related to CAR-T cell therapy, Biomark. Res. 6 (2018) 4.
[33] V. Stolearenco, et al., Cellular interactions and inflammation in the pathogenesis of cutaneous T-cell lymphoma, Front. Cell Dev. Biol. 8 (2020) 851.
[34] C.M. Nicolet, et al., TAG-72-reactive antibody CC49 recognizes molecules expressed by hematopoietic cell lines, Tumour Biol 18 (6) (1997) 356–366.
[35] K.M. Hege, et al., Safety, tumor trafficking and immunogenicity of chimeric antigen receptor (CAR)-T cells specific for TAG-72 in colorectal cancer, J Immunother Cancer 5 (2017) 22.
[36] M.P. Pulitzer, P. Horna, J. Almeida, Sezary syndrome and mycosis fungoides: an overview, including the role of immunophenotyping, Cytometry B Clin Cytom 100 (2) (2021) 132–138.
[37] M. Pulitzer, Cutaneous T-cell lymphoma, Clin. Lab. Med. 37 (3) (2017) 527–546.

[38] S. Samimi, et al., Increased programmed death-1 expression on CD4+ T cells in cutaneous T-cell lymphoma: implications for immune suppression, Arch. Dermatol. 146 (12) (2010) 1382–1388.
[39] M. Battistella, et al., KIR3DL2 expression in cutaneous T-cell lymphomas: expanding the spectrum for KIR3DL2 targeting, Blood 130 (26) (2017) 2900–2902.
[40] A. Pileri, et al., TOX expression in mycosis fungoides and Sezary syndrome, Diagnostics 12 (7) (2022).
[41] A. Yuki, et al., CADM1 is a diagnostic marker in early-stage mycosis fungoides: multicenter study of 58 cases, J. Am. Acad. Dermatol. 79 (6) (2018) 1039–1046.
[42] D. Sommermeyer, et al., Chimeric antigen receptor-modified T cells derived from defined CD8+ and CD4+ subsets confer superior antitumor reactivity in vivo, Leukemia 30 (2) (2016) 492–500.
[43] C.A. Klebanoff, et al., Central memory self/tumor-reactive CD8+ T cells confer superior antitumor immunity compared with effector memory T cells, Proc. Natl. Acad. Sci. U. S. A. 102 (27) (2005) 9571–9576.
[44] Y. Xu, et al., The application of CA72-4 in the diagnosis, prognosis, and treatment of gastric cancer, Biochim. Biophys. Acta Rev. Canc 1876 (2) (2021) 188634.
[45] P.M. Brunner, C. Jonak, R. Knobler, Recent advances in understanding and managing cutaneous T-cell lymphomas, F1000Res 9 (F1000 Faculty Rev) (2020) 331.